Mode Coupling Contribution to Radiation Losses in Curvatures for High and Low Numerical Aperture Plastic Optical Fibers

M. A. Losada, I. Garcés, *Member, IEEE*, J. Mateo, *Member, IEEE*, I. Salinas, J. Lou, and J. Zubía

***Abstract*—We have studied the optical power losses due to multiple curvatures in polymethylmetacrylate (PMMA) plastic optical fibers (POFs) of different numerical apertures (NAs) and attenuation. The fibers were tested for several configurations in order to assess the influence of different types of curved-to-straight fiber transitions in the amount of power radiation. We found that losses are below the standards for all tested fiber types, and thus, they are a suitable choice for local area network (LAN) applications. In addition, our results revealed the presence of modal interactions as confirmed using an experimental procedure to estimate the mode coupling strength for the same fibers.**

***Index Terms*—Curvature losses, mode coupling, plastic optical fiber (POF).**

I. Introduction

PLASTIC OPTICAL fibers (POFs) are being considered for high-performance fiber links at very short distances because of their ductility, light weight, and ease of connection in comparison with those of glass optical fibers (GOFs)[1]–[3]. In addition, POF technology has recently been attracting high interest in data transmission for local area networks (LANs), such as those for home and automobile applications [4], [5].

Two limitations of POFs, however, are evident in house or car environments. First, POFs in market have narrower bandwidths than glass fibers do, which limit their information-carrying capacity even for these short distances. Second, a considerable amount of bending is necessary to install an optical-fiber-based link in these environments, which increases radiation losses [6]–[8].

Low numerical aperture (LNA) fibers have been developed recently with a reduced modal dispersion and, thus, wider bandwidths than the traditional high numerical aperture (HNA) POFs, i.e., those up to 100 MHz in 100 m. According to classical models [6], however, radiation in curvatures should be higher for these LNA POFs because they have more similar core and cladding indexes than HNA fibers have. Therefore, we have studied POF power attenuation in multiple curvatures for different configurations, using POFs of the same core material (i.e., PMMA) but different NAs and attenuation. Our aim was to assess the performance of different types of PMMA fibers submitted to curvatures in order to test their future as a substitute for glass fibers in LAN applications. Thus, we designed a system to estimate the amount of power losses for different curvature configurations when bending HNA and LNA POFs. Although classical models predict higher radiation losses for the LNA fibers, our results show that standard HNA fibers have the higher curvature losses, suggesting the presence of modal interactions [9]. To validate this hypothesis, we estimated the coupling strength of the same fibers used in the bending experiments.

In this paper, we will first describe the experimental system designed to estimate bending losses, as well as the results obtained for three PMMA POFs using several configurations and curvature diameters. We then discuss these results, basing our explanations on modal power transfer, and estimate the mode coupling strength of the same fibers to support our hypothesis. Finally, the conclusions derived from the results of the different experiments are summarized.

II. Experimental Setup

The system used to measure the attenuation in the multiple curvatures consists of a transmitter (model S760) based on a light emitting diode (LED) emitting at 665 nm, with a measured NA of 0.3 and an optical power meter (model FM300) with a *silicon* detector, both from Fotec. Fig. 1 shows this system for one of the configurations of the mandrels, which are, in fact, cylinders with steps of decreasing diameters, as shown in the figure. In all cases, a 4-m fiber length was used, leaving 1 m straight before bending the fiber around the mandrels.

In order to test the behavior of the fibers with different numbers of and types of transitions, seven different configurations of the mandrels have been used, from a maximum of 4 mandrels to 1 mandrel, as shown in Fig. 2.

Configurations 1.1 and 1.2 have one quarter-of-a-turn followed by one straight segment. Thus, they have two transitions for each quarter-of-a-turn: one straight-to-curved and the other curved-to-straight. Both configurations are equivalent and only differ in that, for configuration 1.1, the turning direction is always the same, whereas it alternates for configuration 1.2. Configurations 2.1 and 2.2 have two quarters-of-a-turn followed by a straight segment. The turns have the same direction for configuration 2.1 and alternating directions for configuration

Manuscript received November 27, 2001; revised February 11, 2002. This work was supported by the Comisión Interministerial de Ciencia y Tecnología (CICYT) under Grant TIC2000-0590 and CICYT-FEDER under Grant 2FD97-1070TEL.

M. A. Losada, I. Garcés, J. Mateo, I. Salinas, and J. Lou are with the Grupo de Tecnologías de las Comunicaciones, Departamento de Ingeniería Electrónica y Comunicaciones, Centro Politécnico Superior, Universidad de Zaragoza, María de Luna, 3, 50015 Zaragoza, Spain (e-mail: alosada@posta.unizar.es).

J. Zubía is with the Universidad del País Vasco, Bilbao, Spain.

Publisher Item Identifier 10.1109/JLT.2002.800377.

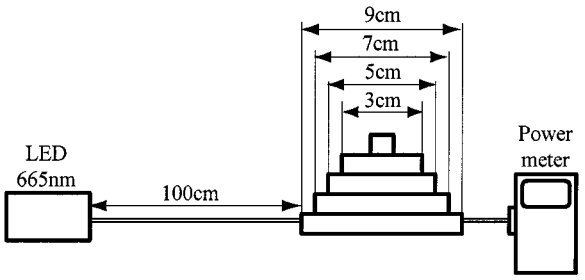

Fig. 1. Setup to obtain curvature losses in POFs, including a diagram of the mandrel used for the experiments with diameters from 3 cm to 9 cm.

2.2, but both have one transition per quarter-of-a-turn. Configuration 3 has only pure curvatures and no intermediate transitions. Finally, configurations 4.1 and 4.2 have one complete turn followed by a straight segment, and thus, half a transition per quarter-of-a-turn. As in the other cases, turns in configuration 4.1 have the same direction, wheras they alternate in configuration 4.2.

The POFs used in the experiments all had a 1-mm-diameter core of PMMA with a step-index profile. The HFBR-RUS500 fiber from Hewlett-Packard has a NA of 0.47, whereas the PMU-CD1002-22-E fiber from Toray with an improved bandwidth has an NA of 0.32. Attenuation was measured by the cutback method for both fibers, yielding similar values of 0.22 and 0.20 dB/m for the HNA and LNA POFs, respectively. In addition, we tested a PGU-CD1001-22E, also from Toray. This fiber has an HNA of 0.5, but it is an upper-grade (U-grade) fiber with a lower attenuation of 0.18 dB/m. In all cases, the core refractive index was 1.492.

We also measured the coupling coefficient by obtaining the images of the near-field output power distributions. The system consisted of an optomechanical setup and a computer-controlled charged-coupled device (CCD) camera. The source was a He–Ne laser (633 nm) launched directly into the front end of the fiber, which was mounted onto a rotating stage to allow input-angle variation. The output intensity was directly imaged on the CCD as shown in Fig. 3.

For a given fiber, the experimental procedure was as follows: First, a fiber between 20 m and 30 m long was placed around an 18-cm diameter reel to avoid small curvatures that can bias the results [10]. Then, the polished fiber ends were mounted on specifically designed chucks, and the launch end was carefully centered in the rotating stage to allow variation of the launch angle in 1° steps. An image was recorded for each input angle and processed in order to obtain the launch angle for which the output pattern changes from disk to ring, known as the transition angle θ_t. Once the angle scan was completed, a determined length of the fiber was cut from the further end, and the whole procedure was repeated. Then, we followed Gloge's power-flow equation [11], [12] to derive a log–log relation between transition angle (θ_t) and fiber length (z) in order to obtain the mode-conversion coefficient D by fitting a log–log plot of the data with a straight line of a half-slope, as follows:

$$\log(\theta_t) = \tfrac{1}{2}\log(z) + \log(2D^{1/2}). \quad (1)$$

III. Results

Preliminary experiments were performed to evaluate the influence of the distance between mandrels, varying this distance up to 75 cm. The results show that separating the mandrels more than 10 cm is irrelevant, suggesting that modal equilibrium after the curved-to-straight transition can be achieved in only 10 cm. The losses for each fiber were obtained for the four curvature radii and the seven configurations depicted in Fig. 2 by rolling it in quarter-of-a-turn steps, up to four complete turns. For each fiber type, several measurements were performed with each of three different 4-m segments to minimize the variability of the results.

As expected, the curvature losses increase when the curvature radius decreases. For all fiber types, we found that configurations with curvatures in a single direction present similar losses to those with curvatures in both directions, provided they have the same number of straight-to-curved transitions. In this way, configurations 1.1 and 1.2, which have two transitions per quarter-of-a-turn, are equivalent, as are configurations 2.1 and 2.2 as well as 4.1 and 4.2, respectively.

In addition, it is clear from the data that the configurations with the greater number of transitions have the higher losses. In this way, the lower losses are found for configuration 3, with no intermediate transitions, followed by configurations 4.1 and 4.2, with half a transition per quarter-of-a-turn ,and then by configurations 2.1 and 2.2, with one transition per quarter-of-a-turn.

The configurations with the higher losses are configurations 1.1 and 1.2. To illustrate this behavior, the increase of losses when bending the HNA fiber around 5-cm-diameter mandrels is shown in Fig. 4. For the sake of simplicity, the results for configurations 1.1 and 1.2, 2.1 and 2.2, and 4.1 and 4.2 have been averaged respectively. The figure shows how the losses increase steadily with the number of turns, up to four complete turns, without reaching a saturation value, although this increase is flatter for those configurations with less transitions.

Thus, we found that the losses for a configuration are higher as the number of transitions increases for a given number of turns. This fact is true for all fiber types and radius sizes, although the absolute value of the loss is different. In fact, our measurements show lower losses for the LNA fiber than for the standard HNA fiber for all the situations tested, except for configuration 3 with 7-cm and 9-cm diameters. The losses for the U-grade HNA fiber are, however, even lower than those obtained for the LNA fiber. We have also observed that the standard HNA fiber losses increase more steeply with increasing turns than do the losses for the other fiber types. This is true for all the configurations and radii tested.

To quantify this effect, we have obtained linear fits of the curvature losses for all configurations with a 2.5-cm radius for both the standard HNA and the LNA fibers. An average of the slopes for all configurations gives a value of 0.028 for the standard HNA, whereas for the LNA fiber, the value is only 0.019.

To summarize our results for the studied fiber types, we show in Fig. 5 the losses when bending the fibers two-and-a-half turns around the mandrels in configuration 1.1 as curvature radius increases. Because this is the configuration with the higher losses,

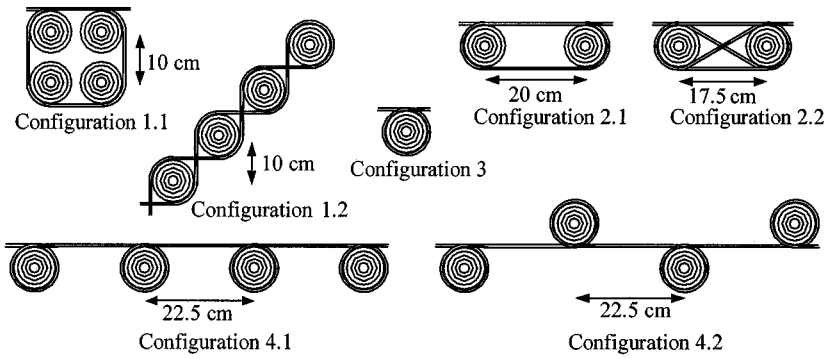

Fig. 2. Mandrel configurations tested in the experiments.

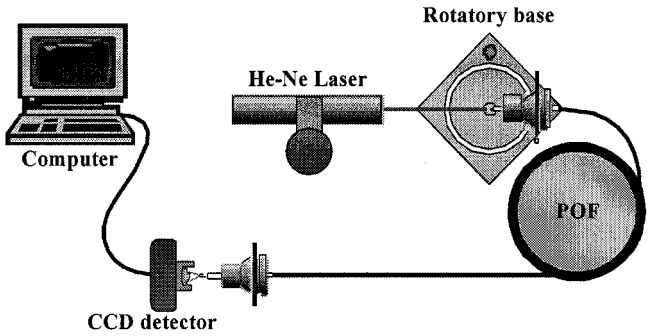

Fig. 3. Experimental setup used to obtain the power distribution images.

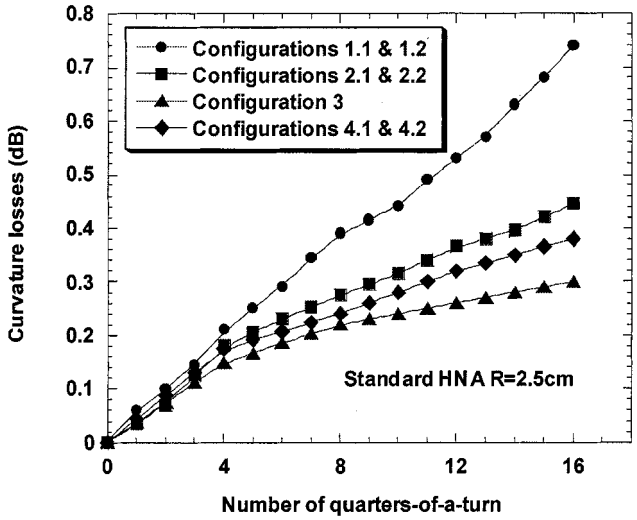

Fig. 4. HNA POF curvature losses as a function of the number of quarters-of-a-turn for a mandrel diameter of 5 cm.

we can conclude that they are always below 0.5 dB for curvature radii equal or greater than 2.5 cm. Similar results have been obtained by other researchers [7]. The losses, however, increase very steeply for smaller radii. The figure also shows how curvature losses are higher for the standard HNA fiber.

IV. Discussion

We have tested three kinds of PMMA POFs of different NAs and attenuation to assess their behavior when they are bent, which occurs frequently in home or automobile applications. Our results show that losses for 16 quarters-of-a-turn are lower

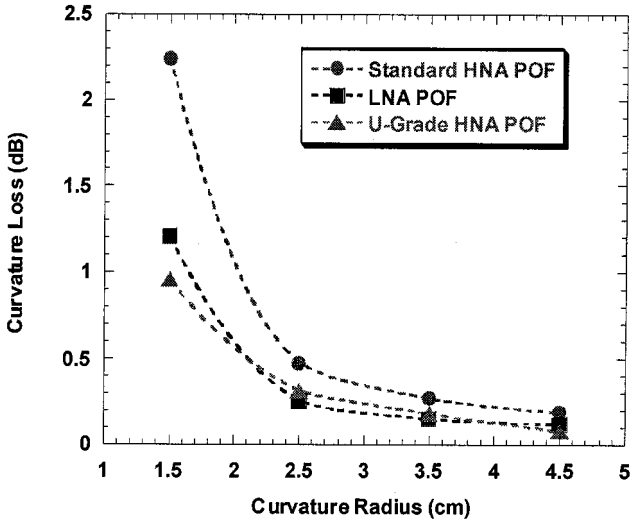

Fig. 5. Losses for the HNA and LNA POFs for configuration 1.1 in 10 quarters-of-a-turn and curvature radii ranging from 1.5 cm to 4.5 cm.

than 1 dB for all fibers and all configurations tested when the curvature diameter is equal to or greater than 5 cm. In addition, none of the fibers present losses higher than 0.5 dB for 10 quarters-of-a-turn over a curvature diameter of 5 cm. In this way, all fibers tested are below the limits set by the ATM-Forum Standard AF-PHY-0079.001 that was defined only for LNA fibers, because they have wider bandwidths. Thus, LNA POFs can be used for 50-m links at 155 Mb/s, which is another of the latter standard requirements that cannot be met by standard HNA POFs. In conclusion, LNA PMMA POFs are a very suitable alternative to GOFs for LAN applications.

We found in most cases lower bending losses for the LNA fiber than for the standard HNA fiber with similar attenuation. Only for configuration 3 with the two larger radii are the standard HNA losses lower. For all other configurations, and even for configuration 3 with the radius smaller than 3.5 cm, the losses are larger for the HNA fiber. However, fiber losses are even slightly lower for the U-grade HNA than for the LNA fiber in all cases.

Traditional models postulate that, as the geometry changes for a bent fiber, some of the formerly propagating rays change to refracted ones and, thus, part of the energy traveling through the fiber is radiated. The energy proportion transferred from bounded toward leaky rays depends on the critical angle, being

higher for lower angles; thus, the lower the NA, the higher the curvature losses [6]. Therefore, this theory predicts higher losses for the LNA fiber and cannot explain part of our results, making it necessary to use a more complex model including modal power transfer.

Modal theory postulates two different effects to account for bending losses: transition losses and curvature losses. Transition losses occur because the modal patterns meeting the geometrical constrains in a straight fiber are different than the modal patterns meeting those in a bent one [13]. This pattern adjustment involves a power loss, which is independent from the losses in the curvature itself.

Using this theory, the differences we found among the results for different configurations tested can be justified. First, for a given curvature radius, we found smaller losses for configuration 3 with only pure curvatures and no transitions, and losses subsequently higher for those configurations with a greater number of transitions. According to the model, these extra losses can be attributed to pattern adjustment in the transitions, which is also supported by the fact that we found similar losses for a given fiber when the number of transitions per turn was the same, independent of the turning direction.

To explain the greater power loss in the standard HNA fiber, we suggest that a stronger mode coupling in this fiber type [9], [14] could compensate the power radiated in the curvatures by supplying energy to higher order modes from lower order modes. In this way, the power transfer from lower to higher modes will be small for a fiber with a weak mode coupling, whereas, for a fiber with a high coupling strength, a considerable amount of power is transferred from lower to higher order modes, increasing the total loss. This effect can be related to the fact that curvature losses increase more steeply with the number of turns for the standard HNA fiber than for the other fibers. This effect has been quantified by calculating the average slope of the curvature losses versus number of turns, which is significantly higher for the standard HNA fiber.

To find further support for our hypothesis, we measured the coupling strength by recording the changes of fiber output power with mode coupling. When the optical power in a POF reaches the equilibrium modal distribution, the far field presents a disk pattern, which changes to a ring pattern when mode coupling is incomplete. This method was first proposed by Gambling *et al.* [12] for GOFs and has been applied later to POFs by other authors [9].

The mode-conversion coefficient D is related to the coupling coefficient, which is a measure of coupling strength, and is greater when mode coupling is stronger. In Fig. 6, we plot in log–log coordinates the transition angle in radians for all fiber types versus fiber length in meters. Each point is the average of at least three measurements. Data was fitted to the straight line defined in (1) using the direct-search method and leaving the slope and the intercept as degrees of freedom.

As in a previous work [14], we found a good agreement with the model, as all slopes were near 0.5 for all fiber types. In that study, we also found a similar D value for our standard HNA and that obtained by Garito *et al.* [9] for a PMMA fiber with similar characteristics. The values of the mode-conversion constant, calculated from the intercept, as well as their standard deviations are shown in Table I.

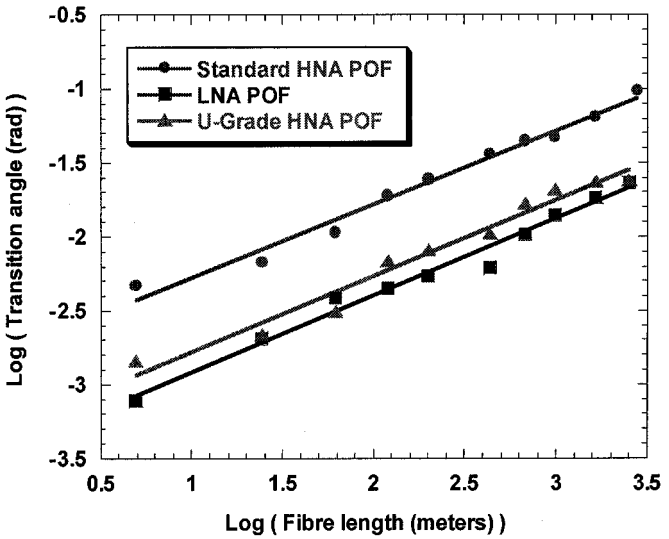

Fig. 6. Transition angle versus fiber length obtained for the LNA fiber (circles) and for the HNA fiber with high attenuation (squares) and low attenuation (triangles).

TABLE I
MODE CONVERSION CONSTANTS AND THEIR STANDARD DEVIATIONS FOR THE STUDIED FIBER TYPES

Type	$D\ (rad^2/m)$	σ_D
S-HNA	8.7×10^{-4}	1.2×10^{-4}
U-HNA	3.3×10^{-4}	2.6×10^{-5}
LNA	2.8×10^{-4}	3.5×10^{-5}

The values of D show that mode coupling is significantly higher for the standard fiber with HNA than for the others. The values of D for the LNA and the U-grade HNA are, however, very similar. Because both the LNA and the U-grade HNA fibers show a similar behavior for curvatures, it seems reasonable to think that there is a contribution of mode coupling to curvature losses. In this way, our results for coupling strength support the hypothesis of a compensation of optical power, suggesting that optical power can be transferred from lower to higher order modes, increasing the amount of power radiated in the curvatures.

V. CONCLUSION

We show in this paper that PMMA POFs of different types have curvature losses lower than the limits set by the current standard. Thus, they are a suitable alternative to GOFs in LAN applications. We have tested several configurations and concluded that those with the same number of transitions present similar losses. We tested three types of PMMA fibers with different NAs and attenuation: a standard HNA POF, a wide-bandwidth LNA POF with an attenuation similar to the latter, and finally, a U-grade HNA POF with lower attenuation. Curvature losses were higher for the standard HNA POF, whereas they were very similar for the other types. We estimated mode coupling strength for the three POFs in order to explain our results

and found that mode coupling is stronger for the standard HNA POF, followed by the U-grade HNA POF, and that the LNA fiber has a weaker coupling. Thus, we conclude that mode coupling contributes appreciably to higher curvature attenuation by compensating radiation losses in higher modes by power transfer from the lower modes.

REFERENCES

[1] Y. Koike, T. Ishigure, and E. Nihei, "High-bandwidth graded index polymer optical fiber," *J. Lightwave Technol.*, vol. 13, pp. 1475–1489, July 1995.

[2] E. Nihei, T. Ishigure, N. Tanio, and Y. Koike, "Present prospect of graded index plastic optical fiber in telecommunications," *IEICE Trans. Electron.*, vol. E-80-c, no. 1, pp. 117–122, 1997.

[3] U. Steiger, "Sensor properties and applications of POF," in *Proc. POF'98, 7th Int. Conf. Plastic Optical Fibers and Applications*, Berlin, Germany, pp. 171–177.

[4] F. Mederer, R. Jäger, P. Schnitzer, H. Unold, M. Kicherer, K. J. Ebeling, M. Naritomi, and R. Yoshida, "Multi-Gb/s grade-index POF data link with butt-coupled single-mode InGaAs VCSEL," *IEEE Photon. Technol. Lett.*, vol. 12, no. 2, pp. 199–201, 2000.

[5] M. Naritomi, "Model home project in Japan using GI-POF," in *Proc. POF'00, 9th Int. Conf. Plastic Optical Fibers and Applications*, Boston, MA, pp. 8–11.

[6] A. A. P. Boechat, D. Su, D. R. Hall, and J. D. C. Jones, "Bend loss in large core multimode optical fiber beam delivery systems," *Appl. Opt.*, vol. 30, no. 3, pp. 321–327, 1991.

[7] J. Marcou and K. Michelet, "A new method to evaluate the bends in polymer optical fibers," in *Proc. POF'96, 5th Int. Conf. Plastic Optical Fibers and Applications*, Paris, France, pp. 205–212.

[8] J. Arrúe, J. Zubía, G. Fuster, and D. Kalymnios, "Light power behavior when bending plastic optical fibers," *Proc. Inst. Elect. Eng. Optoelectron.*, vol. 145, no. 6, pp. 313–318, 1998.

[9] A. F. Garito, J. Wang, and R. Gao, "Effects of random perturbations in plastic optical fibers," *Science*, vol. 281, no. 14, pp. 962–967, Aug. 1998.

[10] G. Durana, J. Zubía, M. Lomer, M. López-Amo, and J. Arrúe, "Wavelength dependence of bending losses on step index POFs," in *Proc. POF 2000, 9th Int. Conf. Plastic Optical Fibers and Applications*, Boston, MA, pp. 184–186.

[11] D. Gloge, "Optical power flow in multimode fibers," *Bell Syst. Tech. J.*, vol. 51, pp. 50–66, 1972.

[12] W. A. Gambling, D. N. Payne, and H. Matsumura, "Mode conversion coefficients in optical fibers," *Appl. Opt.*, vol. 14, no. 7, pp. 1538–1542, 1975.

[13] M. Y. Loke and J. N. McMullin, "Simulation and measurement of radiation loss at multimode fiber macrobends," *J. Lightwave Technol.*, vol. 8, pp. 1250–1255, Aug. 1990.

[14] M. A. Losada, I. Garcés, J. Mateo, I. Salinas, and J. Zubía, "Mode coupling in plastic optical fibers of high and low numerical apertures," in *Proc. POF'01, 10th Int. Conf. Plastic Optical Fibers and Applications*, Amsterdam, Holland, pp. 117–120.

M. A. Losada, photograph and biography not available at the time of publication.

I. Garcés (M'97), photograph and biography not available at the time of publication.

J. Mateo (M'91), photograph and biography not available at the time of publication.

I. Salinas, photograph and biography not available at the time of publication.

J. Lou, photograph and biography not available at the time of publication.

J. Zubía, photograph and biography not available at the time of publication.